



Cite this: *New J. Chem.*, 2018, 42, 17296

New iridium-containing conjugated polymers for polymer solar cell applications

M. L. Keshtov,^a S. A. Kuklin,^a I. O. Konstantinov,^a Fang-Chung Chen,^b Zhi-yuan Xie^c and Ganesh D. Sharma^d*

A series of novel donor–acceptor (D–A) copolymers **P1–P5** with iridium-complexed moieties in their side chains have been synthesized on the basis of a new iridium-containing monomer. The results obtained show that **P1–P5** have good thermal stability (317–347 °C) for photovoltaic applications. These copolymers absorb visible light in a broad spectral range up to 680 nm. The optical bandgaps of **P1–P5** are in the range of 1.96–2.08 eV, respectively. The HOMO and LUMO energy levels of the polymers **P1–P5** estimated from cyclic voltammetry measurements indicate that these copolymers are suitable as electron donors along with PC₇₁BM as an electron acceptor for bulk heterojunction polymer solar cells. BHJ polymer solar cells were developed based on blend compositions (**P1–P5**):PC₇₁BM. The values of J_{sc} , V_{oc} , and FF are in the range of 0.95–4.44 mA cm⁻², 0.67–0.69 V and 34.6–56.8%, and the power conversion efficiencies (PCE) are in the range of 0.22–1.74%, respectively, the highest value of 1.74% being for **P3**. Increase of the photovoltaic parameters was achieved with increasing iridium complex percentage in the polymers due to involvement of triplet effects. The improvement in the efficiency of the triplet-forming polymers **P2** and **P3** in comparison with **P1** appears to be due to the formation of triplet excitons in comparison with singlet excitons in the polymer **P1** which does not contain heavy metals. With further increase in the content of iridium complex fragments in the polymers, for example, up to 3 mol% for polymer **P4**, the efficiency falls to 1.23% and further decreased to 0.22% for **P5**.

Received 9th July 2018,
Accepted 20th September 2018

DOI: 10.1039/c8nj03410a

rsc.li/njc

Introduction

Over the past few years, encouraging progress has been made in the field of polymer solar cells (PSCs) based on a bulk heterojunction (BHJ) active layer¹ as an inexpensive alternative to silicon solar cells due to their unique advantages, such as low cost, light-weight, manufacturability and flexibility of the devices.² In connection with this, great efforts have been made to optimize the spectral characteristics of the conjugated polymers by reducing the optical band gap and optimizing their energy levels. Although many narrow-bandgap polymers have been proposed for photovoltaic applications, the power conversion efficiency (PCE) of single BHJ layer PSCs has now reached about 10–12%,³ which limits their introduction into industrial production (it is believed that the efficiency of PSCs should be about 15% for commercialization).⁴ Although recent advances in the field of

organic photovoltaics are largely based on narrow-bandgap conjugated polymers, it is known that it is difficult to achieve a high efficiency value for practical use on the basis of pure polymers only. One of the reasons limiting the efficiency of PSCs is the short diffusion length of the singlet exciton, which is determined by its mobility and lifetime. One possible approach to increasing the diffusion length of excitons and, as a consequence, the effectiveness of PSCs is the use of triplet-forming organo-metallic polymers. The formation of a large number of charge-transfer triplet states, which have a microsecond lifetime ($\sim 10^{-6}$ s) in comparison with the relatively short nanosecond lifetime ($\sim 10^{-9}$ s) of the singlet state, is attractive for improving the photovoltaic characteristics of PSCs.⁵ A difference of three orders of magnitude can be used to significantly increase the diffusion length of excitons, which is about 5–10 nm in most photovoltaic materials.⁶ In connection with this, interest in the conjugated triplet organo-metallic polymers as donor materials for PSCs has recently grown. In particular, Holdcroft reported a photovoltaic study in which Ir complexes are coordinated with conjugated poly(fluorene-co-phenylpyridine),⁷ where for the PSCs based on poly(9,9-dioctylfluorene-co-tris(2-phenylpyridine)-iridium)(iii) the PCE values increased 35-fold compared to the device based on poly(9,9-dihexylfluorene-co-2-phenylpyridine), which was attributed to

^a Institute of Organoelement Compounds of the Russian Academy of Sciences, Vavilova St., 28, 119991, Moscow, Russian Federation.
E-mail: keshtov@ineos.ac.ru

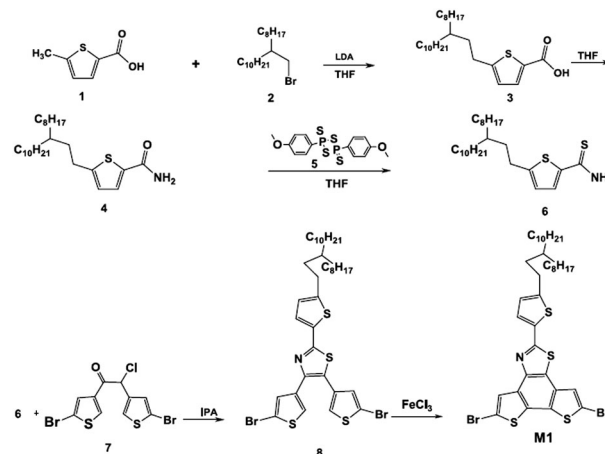
^b Department of Photonics, National Chiao Tung University, Hsinchu 30010, Taiwan
^c Changchun Institute of Applied Chemistry, Chinese Academy of Sciences, Changchun 130022, China

^d Department of Physics, The LNM Institute for Information Technology, Jamdoli, Jaipur, India

the formation of triplet states in the iridium-containing polymers. Yang *et al.* studied mixtures of poly(3-hexylthiophene) (P3HT) with molecular Ir(mppy)₃ using CdSe nanoparticles as an acceptor⁸ and demonstrated an increase in the generation of triplet excitons due to an increase in the degree of singlet–triplet conversion, while the magnitude of the short circuit current (J_{sc}) increased by a factor of two and the value of open circuit voltage (V_{oc}) by 50%, after addition of a triplet metal complex in comparison with a metal-free reference device. In addition, Chen *et al.* recently reported PSCs based on conjugated polymers containing indacenodithiophene and cyclometallated platinum complexes with a maximum power conversion efficiency (PCE) of 2.9%.⁹ Wong *et al.* also demonstrated effective platinopolyine/PC₇₁BM based solar cells, which achieved the highest efficiency among metal-containing conjugated polymers (4–5%).¹⁰ Although platinopolyines of the type *trans*-[Pt(PR₃)₂-C≡C-R-C≡C-]_n attracted considerable attention for use in optoelectronic devices,^{11–14} in most cases their efficiency was low due to the large bandgap width ($E_g > 2.5$ eV), the possible unfavorable arrangement of energy levels and low charge-transport properties. In polyplatinines, where platinum atoms are located in the main chain, the energy overlap of the 5d Pt and 2p C orbitals leads to a significant decrease of the conjugation length compared to similar polyphenylene ethylene polymers.¹⁵ Therefore, organometallic conjugated polymer architectures, other than polyplatinines, deserve attention as donor materials for a better understanding of the role of heavy metal atoms in the formation of triplets in conjugated polymers for possible application in photovoltaics. In the present article, in contrast to the reviewed studies, iridium atoms connected directly to the side chain of macromolecules and do not interfere with delocalization of the excitons along the polymer chain, providing an increase in the diffusion length of excitons, and simultaneously decreasing the width of the bandgap of the polymer. In this regard, the design of metal polymers will be aimed at developing not only phosphorescent triplet polymer materials, but also phosphorescent triplet polymers with a narrow band gap for high-performance PSCs. It is expected that this work will stimulate the further development of new organometallic polymers for photovoltaic applications and help the achievement of high efficiency PSCs with bulk heterojunctions.

Results and discussion

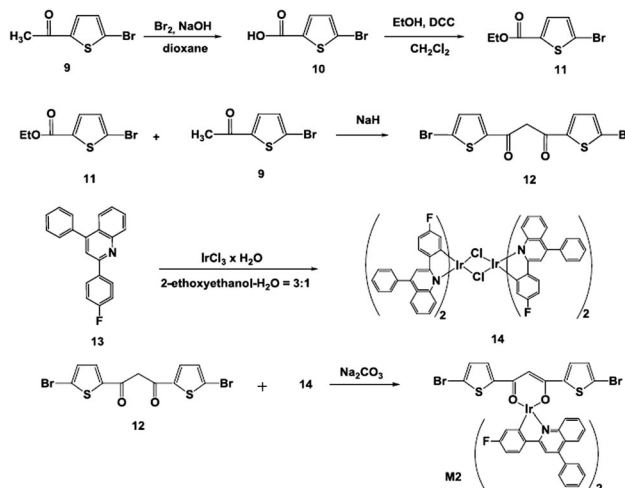
New fused aromatic monomers, (5,8-dibromo-2-[5-(3-octyltridecyl)thiophene-2-yl]bisthiophen-[2-yl]bisthieno[3,2-*e*:2',3'-*g*][1,3]-benzothiazole) (**M1**) and triplet-forming iridium containing bis((2-4-fluorophenyl)-4-phenylquinolino-*C2,N'*)[1,3-bis(5-bromothiophen-2-yl)propan-1,3-dionato-*O,O*]iridium(III) (**M2**) have been synthesized. Monomer **M1** was synthesized by a three stage method including metallalization of 5-methylthiophen-2-carboxylic acid (**1**) with lithium diisopropyl amide with subsequent alkylation of carbanion with 2-octyldodecylbromide (**2**) to give 5-(3-octyldodecyl)thiophene-2-carboxylic acid (**3**) with a yield of 97%.



Scheme 1 Synthetic route of monomer **M1**.

Reaction of the acid **3** with carbonyldiimidazole (CDI) followed by treatment with ammonia solution gave amide **4** with the yield of 95%. The amide **4** was treated with Lowesson reagent (**5**) with formation of thioamide **6**, which was purified by means of column chromatography and obtained with a moderate yield of 57%. Interaction of **6** with an equimolar amount of chloro-ketone **7** led to thiazole derivative **8**, which was obtained with the yield of 64%. Oxidative cyclization of **8** occurs upon treatment with anhydrous FeCl₃ in a dichloromethane–nitromethane solvent mixture and gave targeted monomer **M1** with yield of 79% (as shown in Scheme 1).

Synthesis of bis(2-(4-fluorophenyl)-4-phenylquinolino-*C2,N'*)-[1,3-bis(5-bromothiophen-2-yl)propan-1,3-dionato-*O,O*]iridium(III) (**M2**) was conducted according to Scheme 2; at first, the new ligand, 1,3-bis(5-bromothiophen-2-yl)propan-1,3-dione (**12**) and an intermediate dimer complex (**14**) were prepared. The dione ligand **12** was obtained in a three stage synthesis starting from the oxidation of 2-bromo-5-acetylthiophene (**9**) by sodium hypobromide to yield the acid **10**. In the second stage the acid **10** was converted to its ethyl ester **11** under the action of



Scheme 2 Synthetic routes of monomer **M2**.

dicyclohexylcarbodiimide (DCC) in the presence of dimethylaminopyridine (DMAP). Equimolar amounts of ester **11** and starting compound **9** react in the condensation reaction in the presence of an excess of sodium hydride with formation of 1,3-bis(5-bromothiophen-2-yl)propan-1,3-dione (**12**), which was purified by column chromatography. Reaction of two-molar excess of 2-(4-fluorophenyl)-4-phenylquinoxaline (**13**)¹⁶ in 2-ethoxyethanol with an aqueous solution of IrCl₃·xH₂O gave red-orange intermediate dimer **14** with excellent yield (99%), which was used in the reaction with the dione ligand **12** for preparation of target monomer **M2** with 87% yield.

The compositions and structures of all the intermediate compounds **2–14** and the target monomers **M1** and **M2** were confirmed by elemental analysis data and ¹H and ¹³C NMR spectroscopy. In particular, in the low-field region of the ¹H NMR spectrum of the target monomer **M1** two singlet and two doublet signals were observed at δ 7.87, 7.40, 7.25 and 6.80 ppm with the intensity ratio of 1 : 1 : 1 : 1, which related to the protons of thiophene fragments (Fig. 1). In the up-field region at δ 2.87 ppm a triplet resonance appears typical of a methylene group directly connected to a thiophene ring, and in the range of δ 1.76–0.90 ppm there are signals related to other protons of the aliphatic chains.

The target iridium complex **M2** was characterized by ¹H and ¹³C NMR spectroscopy and elemental analysis, which confirmed its structure and composition. For example, two doublet and one singlet resonances δ = 7.04, 6.88 and 5.66 ppm with the intensity ratio of 2 : 2 : 1 related to the diketone ligand can be observed in the low-field region of the ¹H NMR spectrum. Another nine signals at δ = 8.49 (d, 2H), 7.98 (s, 2H), 7.90 (dd, 2H), 7.82 (d, 2H), 7.60 (m, 10H), 7.35 (t, 2H), 7.28 (m, 2H + CDCl₃), 6.77 (td, 2H), and 6.32 (dd, 2H) are related to protons of 2-(4-fluorophenyl)quinoxaline ligands. The ¹³C NMR spectrum contains six doublet resonances at δ = 162.39 (d, J = 253.1 Hz), 151.82 (d, J = 6.04 Hz), 130.73 (d, J = 21.34 Hz), 127.41 (d, J = 9.46 Hz), 122.10 (d, J = 17.32 Hz), and 108.99 (d, J = 23.47 Hz), and their multiplicity was caused by spin–spin interaction with a fluorine atom. Another singlet signal is related to carbon atoms of

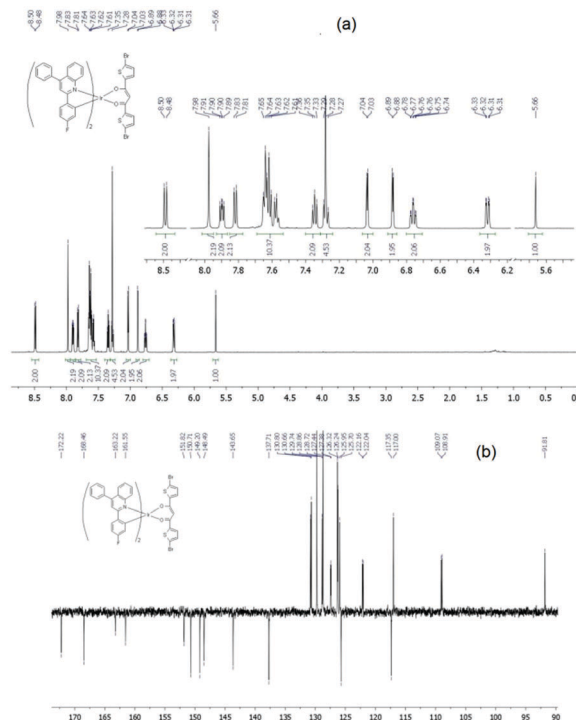


Fig. 2 ¹H (a) and ¹³C (b) NMR spectra of monomer **M2** in CDCl₃.

non-fluorinated fragments of phenylquinoline ligands. The number of signals in the ¹³C spectrum and the integral intensity values in the ¹H spectrum confirm the structure of complex **M2** (Fig. 2).

Based on the monomers **M1**, **M2** and **M3**, we synthesized five new D–A conjugated polymers **P1–P5** with different contents of iridium triplet complexes (0, 0.5, 1.0, 1.5, 3.0 and 100 mol%) in the chain (Scheme 3). In order to maintain the linear structure of the polymer backbone and minimize the charge loss and transport properties of the polymers, the iridium-containing metal complex was inserted into the polymer backbone statistically through the β-diketone auxiliary ligand.

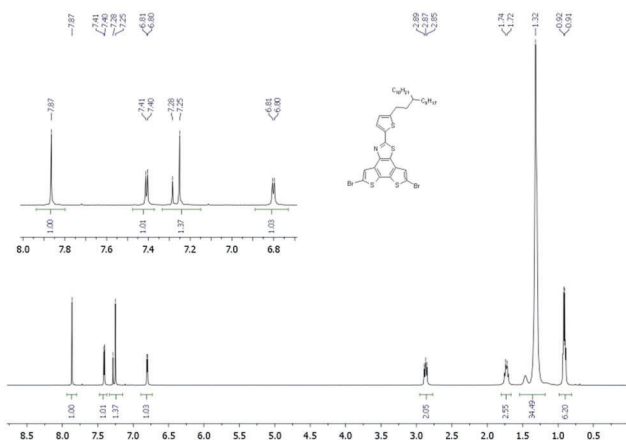
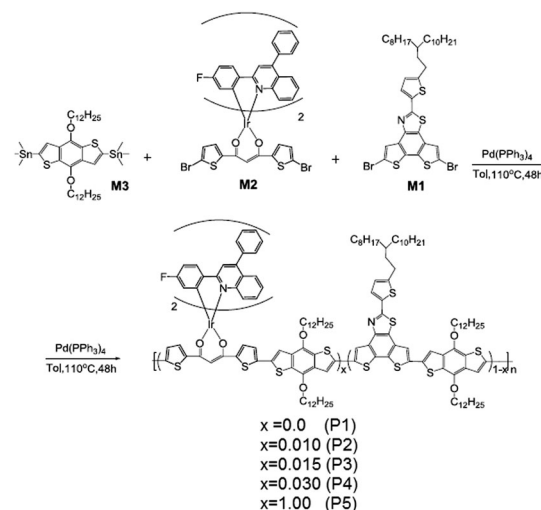


Fig. 1 ¹H NMR spectrum of 5,8-dibromo-2-[5-(3-octyl/tridecyl)thiophen-2-yl]bisthieno[3,2-e',3'-g][1,3]benzothiazole (**M1**).



Scheme 3 Synthetic routes of copolymers **P1–P5**.

Polycondensation was carried out under Stille cross-coupling conditions in boiling toluene using tetrakis(triphenylphosphine)-palladium as the catalyst. The resulting polymers were purified from catalyst residues, and low molecular weight impurities by reprecipitation from solution twice to methanol and subsequent extraction with methanol, hexane, acetone and chloroform. The process proceeded under homogeneous conditions and allowed polymers with high molecular weights to be obtained in the form of a dark purple powder with yields in the range of 69–79%, respectively.

The composition and structure of polymers **P1–P5** are confirmed by the elemental analysis data and ^1H NMR spectroscopy. In particular, there are multiplets in the weak-field region in the range of δ 8.10–6.50 ppm belonging to the aromatic protons of the polymer unit in the ^1H NMR spectrum of the polymer **P1**; in the strong-field region in the range of δ 4.30–2.70 ppm there are two multiplets characteristic of two different CH_2 groups which are directly connected to the thiophene ring and alkoxy group. Signals that belong to the remaining hydrogen atoms of the alkyl substituents are detected within the range of δ 1.47–0.60 ppm (Fig. 3).

Although the proton spectrum of **P2** is complex, the ratio of the integral intensity of the aromatic part to the aliphatic part corresponds to the proposed structure. These results, combined with elemental analysis, show that the reaction process was successful and complete. The number-average molecular weights (M_n) and polydispersity (M_w/M_n) of polymers **P1–P5**, determined by the GPC method, range from 48 700–72 600 and 2.10–3.43, respectively. The polymers are soluble in common organic solvents such as chloroform, THF, and *o*-dichlorobenzene, which made it possible to obtain films based on them for electrochemical and photovoltaic studies. The introduction of low concentrations of Ir into the polymers showed a small effect on their solubility.

Thermal properties

The thermal properties of the polymers **P1–P5** were examined by means of thermogravimetric analysis (TGA); the results are listed in Table 1, and the corresponding TGA curves are shown in Fig. 4. All the polymers exhibit high thermal stability.

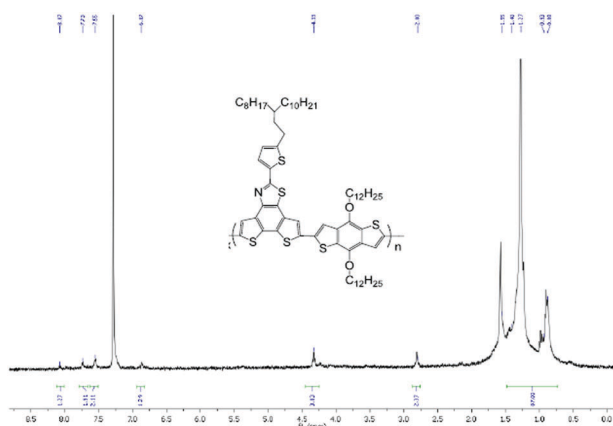


Fig. 3 ^1H NMR spectrum of polymer **P1** in CDCl_3 .

Table 1 Molecular weights and thermal properties of the polymers **P1–P5**

Polymer (Ir, mol%)	Yield (%)	M_n	M_w	M_w/M_n	$T_{5\%}$ ($^\circ\text{C}$)
P1	79	50 100	156 200	3.12	317
P2	77	48 700	109 400	2.25	317
P3	72	54 700	187 500	3.43	330
P4	71	53 500	160 500	3.00	336
P5	69	72 600	232 300	3.20	347

The temperature values of five percent weight loss ($T_{5\%}$) of polymers **P1–P5** in air, found using TGA, range from 317 to 329 $^\circ\text{C}$, respectively (Table 1). These results show that the polymers have a sufficiently high thermal stability for photovoltaic applications and other optoelectronic devices.

Optical properties

The optical properties of polymers **P1–P5** were investigated by UV and visible spectroscopy, and the results are given in Table 2, and the corresponding absorption spectra in chloroform and films are shown in Fig. 5(a and b), respectively. As one can see from the figures, all polymers exhibit two absorption peaks in solution and films, which are characteristic for donor-acceptor copolymers. Absorption peaks at short wavelengths of 360–407 nm in films refer to $\pi-\pi^*$ -transitions of the conjugated chains, while long-wavelength absorption peaks of 552–570 nm are attributes of strong intramolecular charge transfer in the transition state in the donor-acceptor segments, which are the most important for covering the spectrum of solar radiation. Polymers **P1–P4** show almost identical absorption profiles in the range of 350–600 nm, since they have very similar composition with a very low content of iridium containing blocks. On the other hand, polymer **P5** showed a completely different absorption profile due its high percentage of iridium blocks. The absorption maxima in solid films were slightly shifted to the red region in comparison with the solutions and show bathochromic shifts within 10–19 nm due to aggregation, strong interchain interactions and the formation of π -stack structures and better packing of the macromolecules in thin films. The optical band gap (E_g^{opt}) of polymers **P1–P5**, found from the absorption edges of the polymer films by the formula $1240/\lambda_{\text{edge}}$ vary within 1.96–2.08 eV (Table 2).

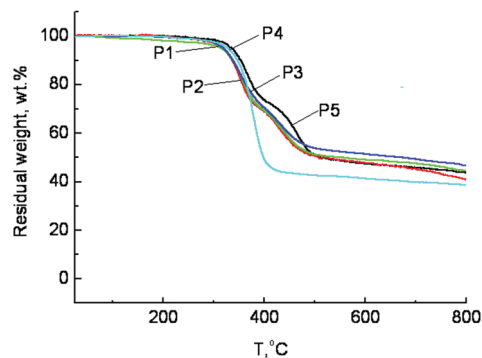
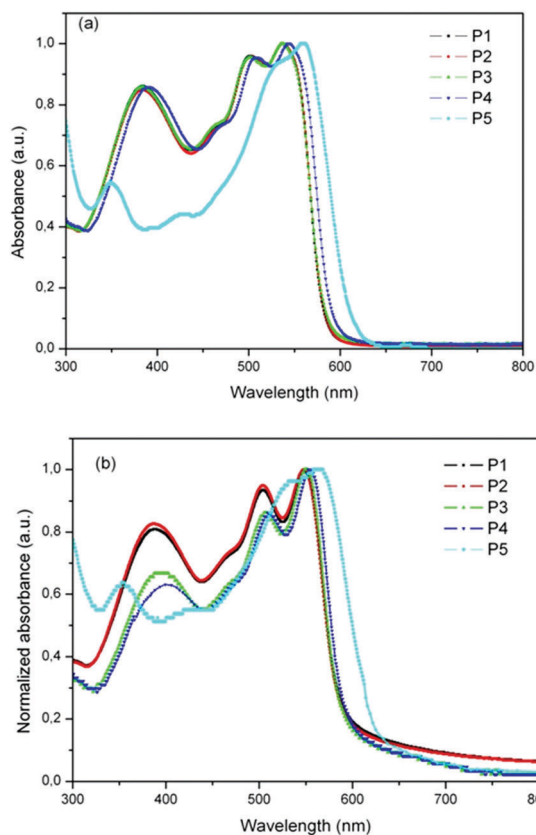


Fig. 4 TGA plots of the polymers **P1–P5** in air at a scanning rate of $50^\circ\text{C min}^{-1}$.

Table 2 Optical and electrochemical properties of the polymers **P1–P5**

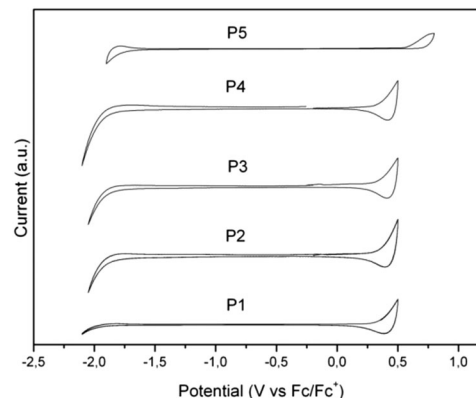
Polymer (Ir, mol%)	$\lambda_{\text{max}}(\text{solution})$ (nm)	$\lambda_{\text{max}}(\text{film})$ (nm)	HOMO (eV)	LUMO (eV)	$E_{\text{g}}^{\text{opt}}$ (eV)
P1	377, 490, 539	390, 500, 552	−5.21	−2.93	2.08
P2	377, 490, 539	390, 500, 552	−5.21	−3.00	2.07
P3	384, 500, 532	407, 513, 558	−5.18	−2.99	2.04
P4	390, 508, 543	401, 501, 555	−5.17	−2.92	2.04
P5	350, 560	360, 570	−5.42	−3.08	1.96

Fig. 5 Normalized absorption spectra of the polymers **P1–P5** in (a) chloroform solution and (b) thin films.

Electrochemical properties

The electrochemical properties of the polymers **P1–P5** were investigated by cyclic voltammetry; the results are given in Table 2, and the corresponding cyclic voltammograms are presented in Fig. 6. Cyclic voltammetry of the polymer films was carried out in acetonitrile with 0.1 M Bu_4NBF_4 at a scan rate of 50 mV s^{-1} . The platinum electrode was used as a counter electrode, Ag/Ag^+ in a 0.1 M solution of silver nitrate was used as a reference electrode, and Fc/Fc^+ was used as an external standard. All the polymers exhibit reversible oxidation–reduction properties. From the onset oxidation ($E_{\text{ox}}^{\text{onset}}$) and reduction ($E_{\text{red}}^{\text{onset}}$) potentials of the polymers, the highest occupied molecular orbital (HOMO) and lowest unoccupied molecular orbital (LUMO) energies and bandgap values of the polymers (E_{g}^{ec}) were calculated according to equations

$$\text{HOMO} = -(E_{\text{ox}}^{\text{ons}} + 4.84) \text{ (eV)},$$

Fig. 6 Cyclic voltammograms of copolymers **P1–P5**.

$$\text{LUMO} = -(E_{\text{red}}^{\text{ons}} + 4.84) \text{ (eV)},$$

$$E_{\text{g}}^{\text{ec}} = (E_{\text{ox}}^{\text{ons}} - E_{\text{red}}^{\text{ons}}) \text{ (eV)}.$$

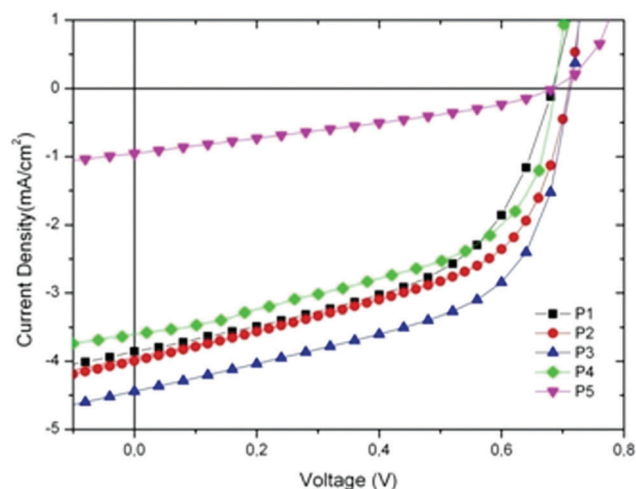
The HOMO and LUMO energies of the polymers **P1–P5** found onset oxidation and reduction potentials, respectively observed in the voltammograms are -5.21 , -5.21 , -5.18 , 5.17 , 5.42 eV, and -2.93 , -3.00 , -2.99 , -2.92 and -3.08 eV, respectively. Polymers **P1–P4** show fairly close HOMO and LUMO levels and a small difference in the energy levels of the HOMO and LUMO suggests a slight effect of the inclusion of iridium complexes. All the polymers exhibit low-lying HOMO levels within (-5.42) – $(-5.18$ eV), which favors a high open circuit voltage, since usually V_{oc} is proportional to the difference between the HOMO level of the polymer (donor) and the LUMO level of fullerene (acceptor). The difference between the LUMO of the polymers and the LUMO of PC_{71}BM (-4.2 eV) varies between 1.12 and 1.27 eV. These energy offset values are greater than 0.3 eV, which is the generally accepted minimum driving force for efficient separation of the excitons into free charge carriers.

Photovoltaic properties

In order to evaluate the influence of triple-forming iridium complexes on the photovoltaic characteristics of PSCs, bulk heterojunction polymer solar cells with a structure of ITO/PEDOT-PSS/copolymer:PC₇₁BM/Ca/Al were created on the basis of the polymers **P1–P5**. The main parameters of the PSCs are given in Table 3, and the corresponding J – V characteristics are shown in Fig. 7. The short circuit current density (J_{sc}), the open circuit voltage (V_{oc}) and the filling factor (FF) of the PSCs based on **P1–P5** vary within the ranges of 0.95–4.44 mA cm^{-2} ; 0.67–0.69 V and 34.6–56.8%, and the efficiency (PCE) in the range 0.22–1.74%, respectively (Table 3). The value of V_{oc} for all the devices is almost the same due to the similar values of HOMO energy levels of the copolymers. However, the PCEs of the PSCs are different, mainly due to the different values of J_{sc} and FF. With an increase of the triplet iridium complex concentration from 0 to 1.5%, the photovoltaic performance increases due to the participation of the triplet effect. The device

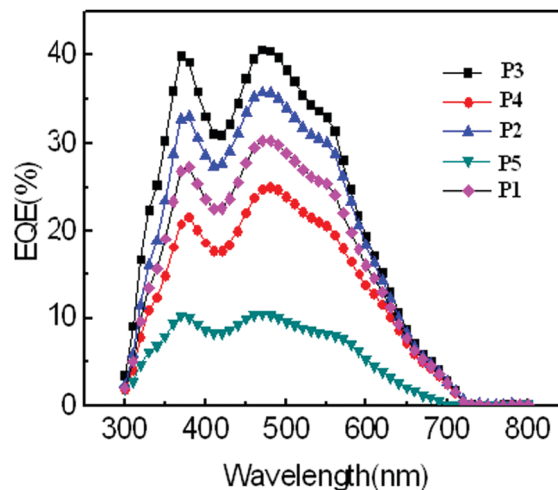
Table 3 Photovoltaic performance of PSCs with the polymers **P1–P5**

Polymer (Ir, mol%)	(V_{oc}) (V)	(J_{sc}) (mA cm^{-2})	(FF) (%)	PCE (%)
P1 (0.0)	0.67	3.86	51.8	1.34 (± 0.02)
P2 (1.0)	0.69	4.00	52.9	1.46 (± 0.02)
P3 (1.5)	0.69	4.44	56.8	1.74 (± 0.03)
P4 (3.0)	0.67	3.60	51.0	1.23 (± 0.03)
P5 (100)	0.67	0.95	34.6	0.22 (± 0.01)

**Fig. 7** J - V plots of the PSCs under illumination based on polymers **P1–P5**:PC₇₁BM thin films.

based on the polymer **P3** shows the greatest efficiency equal to 1.74%. Apparently, this is due to higher values of J_{sc} and FF of this device. The improvement in the efficiency of the triplet-forming polymers **P2** and **P3** in comparison with the polymer **P1** is apparently due to the formation of triplet excitons in comparison with singlet excitons in the polymer **P1** containing no heavy metals.

Triplet-forming polymers prevent the recombination of the germinal pairs, have a longer exciton lifetime and, as a consequence, a longer exciton diffusion length, thereby increasing the percentage of excitons reaching the donor/acceptor interface, that is, the efficiency of charge generation and photocurrent generation increases. Indeed, the triplet-forming polymers **P2** and **P3** containing heavy metals exhibit larger values of J_{sc} at an almost identical value of V_{oc} and FF compared to **P1** (Table 3). With further increase in the content of triplet iridium complexes in the polymers, for example, up to 3 mol% for polymer **P4**, the efficiency drops to 1.23%. Photovoltaic characteristics of the device (PCE, J_{sc} , FF) based on **P5** with 100 mol% Ir complex content decreased to a minimum value of 0.22%, 0.95 mA cm^{-2} and 34.6%, respectively. This may be due to the bad charge transfer of the static iridium complex, which destroys the polymer conjugated chain and further reduces the mobility of charges so reducing the short-circuit current in the device. The efficiency of **P1–P5** is lower than that for most known polymer:fullerene systems based on the generation of singlet exciton charges, but this is probably due to the unfavorable absorbing power of **P1–P5**. The external

**Fig. 8** EQE spectra of the PSCs under illumination based on polymers **P1–P5**:PC₇₁BM thin films.

quantum efficiency (EQE) spectra of the devices are shown in Fig. 8. It can be seen from this figure that the EQE spectra consist of two bands *i.e.* a shorter wavelength region peak around 384 nm, which corresponds to the absorption of PC₇₁BM, and another band in the wavelength region (480–700 nm), which corresponds to the absorption band of the polymers. This indicates that both PC₇₁BM and polymers contribute to the exciton generation and thereby photocurrent generation. Moreover, the EQE values are well consistent with the J_{sc} values of the corresponding PSCs. Further improvement in efficiency is expected when optimizing the content of iridium in these systems and selecting D–A conjugated polymers with a wider absorption spectrum covering the entire spectrum of solar radiation.

Device fabrication and testing

PSCs were fabricated on patterned indium tin oxide (ITO)-coated glass substrates. The ITO-coated glass was treated with UV ozone prior to use. Poly(3,4-ethylenedioxythiophene)–poly(styrene-sulfonate) (PEDOT:PSS) was spin coated onto the glass substrates and then baked at 120 °C for 1 h. The photoactive layer, prepared from a blend of different polymers and P₇₀CBM (1:2, w/w) in 1,2-dichlorobenzene, was spin-coated onto the PEDOT:PSS layers. Note that 3% (v/v) 1,8-diiodooctane (DIO) was added in the solution to improve the morphology of the active films. The wet film underwent solvent annealing in a glass Petri dish for at least 10 min before transfer to the thermal evaporator. Then, the device cathode, consisting of Ca (30 nm) and Al (100 nm), was thermally deposited to complete the device fabrication. The J - V (current density–voltage) characteristics of the PSCs were measured using a Keithley 2400 source-measure unit. The photocurrent was measured under illumination from a 150 W Thermal Oriel solar simulator (AM 1.5G). The intensity of the light source was corrected using a standard Si photodiode. The IPCE measurement system (Enli Technology) comprised a quartz tungsten halogen (QTH) lamp as the light source, a monochromator,

an optical chopper, a lock-in amplifier, and a calibrated silicon photodetector.

Conclusions

We have synthesized five D–A copolymers based on various moles of iridium-complexed moieties in their side chain and their optical and electrochemical properties were investigated. These copolymers exhibit medium optical bandgap in the range of 1.96–2.08 eV and suitable HOMO and LUMO energy level matching with the PC₇₁BM. These copolymers were used as an electron donor along with PC₇₁BM as an electron acceptor for their potential application in solution processed PSCs. The highest value of PCE (1.74%) was obtained for the P3 based polymer solar cell. They are primarily investigated without any treatment of the active layer. We expect that the value of PCE can be improved further after adding a solvent additive, thermal annealing, solvent annealing and a combination of these to improve the active layer morphology. Work in this direction is under progress and will be communicated later on.

Conflicts of interest

There are no conflicts to declare.

Acknowledgements

This work was supported by the Russian foundation for basic research (grant number 17-53-53198).

References

- (a) G. Yu, J. Gao, J. C. Hummelen, F. Wudl and A. J. Heeger, *Science*, 1995, **270**, 1789–1791; (b) J. J. M. Halls, C. A. Walsh, N. C. Greenham, E. A. Marseglia, R. H. Friend, S. C. Moratti and A. B. Holmes, *Nature*, 1995, **376**, 498–500.
- (a) L. Lu, T. Zheng, Q. Wu, A. M. Schneider, D. Zhao and L. Yu, *Chem. Rev.*, 2015, **115**, 12666–12731; (b) L. Dou, Y. Liu, Z. Hong, G. Li and Y. Yang, *Chem. Rev.*, 2015, **115**, 12633–12665; (c) H. Yan, L. Ye, S. Li, S. Zhang and J. Hou, *Chem. Rev.*, 2016, **116**, 397–7457; (d) G. J. Hadley, A. Ruseckas and I. D. W. Sumuel, *Chem. Rev.*, 2017, **117**, 796–837; (e) A. J. Heeger, *Adv. Mater.*, 2014, **26**, 10–28.
- (a) S. Li, L. Ye, W. Zhao, S. Zhang, S. Mukherjee, H. Ade and J. Hou, *Adv. Mater.*, 2016, **28**, 9423–9429; (b) L. Huo, T. Liu, X. Sun, Y. Cai., A. J. Heeger and Y. Sun, *Adv. Mater.*, 2015, **27**, 2938–2944; (c) Y. Liu, J. Zhao, Z. Li, C. Mu, W. Ma, H. Hu, K. Jiang, H. Lin, H. Ade and H. Yan, *Nat. Commun.*, 2014, **5**, 5293; (d) S. H. Liao, H. J. Jhuo, P. N. Yeh, Y. S. Cheng, Y. L. Li, Y. H. Lee, S. Sharma and S. A. Chen, *Sci. Rep.*, 2014, **4**, 6813; (e) Z. He, C. Zhong, S. Su, M. Xu, H. Wu and Y. Cao, *Nat. Photonics*, 2012, **6**, 591–595; (f) V. Vohra, K. Kawashima, T. Kakara, T. Koganezawa, I. Osaka, K. Takimiya and H. Murata, *Nat. Photonics*, 2015, **9**, 403; (g) S. Zhang, L. Ye and J. Hou, *Adv. Energy Mater.*, 2016, **6**, 1502529; (h) W. Zhao, D. Qian, S. Zhang, S. Li, O. Inganäs, F. Gao and J. Hou, *Adv. Mater.*, 2016, **28**, 4734–4739; (i) C. Liu, C. K. Yi, K. Wang, Y. Yang, R. S. Bhatta, M. Tsig, S. Xiao and X. Gong, *ACS Appl. Mater. Interfaces*, 2015, **7**, 4928–4935; (j) H. Q. Zhou, Y. Zhang, C. K. Mai, S. D. Collins, G. C. Bazan, T. Q. Nguyen and A. J. Heeger, *Adv. Mater.*, 2015, **27**, 1767–1773; (k) J. Zhao, Y. Li., G. Yang, K. Jiang, H. Lin, H. Ade, W. Ma and H. Yan, *Nat. Energy*, 2016, **1**, 15027.
- K. M. Coakley and M. D. McGehee, *Chem. Mater.*, 2004, **16**, 4533–4542.
- M. A. Baldo, D. F. O'Brien, Y. You, A. Shoustikov, S. Sibley, M. E. Thompson and S. R. Forrest, *Nature*, 1998, **395**, 151–154.
- D. E. Markov, *Phys. Rev. B: Condens. Matter Mater. Phys.*, 2005, **72**, 045217.
- G. L. Schulz and S. Holdcroft, *Chem. Mater.*, 2008, **20**, 5351–5355.
- C. M. Yang, C. H. Wu, H. H. Liao, K. Y. Lai, H. P. Cheng, S. F. Horng, H. F. Meng and J. T. Shy, *Appl. Phys. Lett.*, 2007, **90**, 133509.
- C. Y. Liao, C. P. Chen, C. C. Chang, G. W. Hwang, H. H. Chou and C. H. Cheng, *Sol. Energy Mater. Sol. Cells*, 2013, **109**, 111–119.
- W. Wong, X. Z. Wang, Z. He, A. B. Djurišić, C. T. Yip, K. Y. Cheung, H. Wang, C. S. K. Mak and W. K. Chan, *Nat. Mater.*, 2007, **7**, 521.
- J. S. Wilson, A. S. Dhoot, A. B. Seeley, M. S. Khan, A. Köhler and R. H. Friend, *Nature*, 2001, **413**, 828–831.
- I. Manners, *Science*, 2001, **294**, 1664–1666.
- F. Guo, Y. G. Kim, J. R. Reynolds and K. S. Schanze, *Chem. Commun.*, 2006, 1887–1889.
- A. D. Kohler and D. Beljonne, *Adv. Funct. Mater.*, 2004, **14**, 11–18.
- E. E. Silverman, T. Cardolaccia, X. M. Zhao, K. Y. Kim, K. Haskins-Glusac and K. S. Schanze, *Coord. Chem. Rev.*, 2005, **249**, 1491–1500.
- M. L. Keshtov, E. I. Maltsev, D. V. Marochkin, D. A. Lypenko, S. A. Kuklin, A. F. Smol'yakov and A. R. Khokhlov, *Polym. Sci., Ser. B*, 2014, **56**, 77–88.